

Synthesis and characterization of iron nanoparticles using leaves extract of *Phyllanthus amarus* and its application in crystal-violet degradation

Chinedu Chidi Okpalihu^{1*}, Christopher Alisa², Ali Bilar³, Jennifer Nneamaka Ibekilo⁴

^{1,2,3,4}Department of Chemistry, Federal University of Technology, Owerri, Imo State, Nigeria

email: chineduokpalihu25@gmail.com

Abstract

Nanomaterials play a crucial role in the photocatalytic degradation of dyes in wastewater. In this study, iron oxide nanoparticles (Fe_3O_4 -NPs) were synthesized via a green approach using *Phyllanthus amarus* leaf extract and evaluated for their effectiveness in degrading crystal violet, a common cationic dye. The novelty of this work lies in the dual functionality of *P. amarus* extract as both reducing and capping agent, offering a sustainable and eco-friendly alternative to conventional physical and chemical synthesis methods. Fresh *P. amarus* leaves harvested from the Federal University of Technology Owerri were processed into aqueous extract and reacted with 0.01 M $\text{FeCl}_3 \cdot 6\text{H}_2\text{O}$ in a 1:1 volume ratio, leading to a rapid color change indicating nanoparticle formation. The synthesized nanoparticles (PaFeNPs) were characterized using UV-Vis spectroscopy, X-ray diffraction (XRD), Scanning Electron Microscopy (SEM), and Transmission Electron Microscopy (TEM). UV-Vis analysis revealed a characteristic absorption peak at 286 nm due to surface plasmon resonance. XRD confirmed the presence of Fe_3O_4 with an average crystallite size of ~9.13 nm, while SEM and TEM revealed irregular morphologies and an average particle size of ~86.2 nm, indicating aggregation due to magnetic interactions. The photocatalytic activity of PaFeNPs was tested under UV and dark conditions. Results showed up to 89% degradation of crystal violet within 90 minutes under UV light, significantly outperforming the dark condition, thereby confirming their light-assisted catalytic potential. The presence of bioactive phytochemicals such as flavonoids, terpenoids, and reducing sugars in the extract contributed to the efficient synthesis and stabilization of the nanoparticles. This study demonstrates the feasibility of *Phyllanthus amarus*-mediated green synthesis of iron oxide nanoparticles as a cost-effective, environmentally safe, and scalable solution for industrial dye remediation.

Keywords: Crystal Violet dye Iron, Iron Oxide, Nanoparticles, Phyllanthu Amarus, Crystal Violet dye.

Introduction

In recent years, nanotechnology has rapidly developed into a pioneering and advanced field with a diverse range of applications across various sectors. This expansive domain includes nanomaterials, nanotools, and nanodevices Kamzin et.al (2018). Within the realm of nanomaterials, nanoparticles have attracted the most research attention due to their ease of production and versatility (Machado et.al, 2015). Traditionally, nanoparticles have been synthesized using physical and chemical techniques; however, these methods have limitations, prompting a shift in research toward the creation of

environmentally friendly and sustainable synthesis approaches (Ebrahimi and Mansoori, 2014).

Green Chemistry becomes an eye-catching topic of interest in the past few years because it is a comfortable, secure, inexpensive, and eco-friendly way of synthesis (Dinali et.al, 2017). Iron oxide nanoparticles with different morphologies and sizes have been extensively studied due to their broad applications. Iron oxide nanoparticles (FeNPs) have drawn interest in antimicrobial and antilarvacidal studies (Machado et.al, 2015). The present research work reveals a simplified and less expensive method of iron oxide nanoparticles synthesis (green synthesis) from plant extracts that have medicinal potential against anemic red blood cells.

The core potential of nanoscience and nanotechnology is demonstrated by the fact that the properties of materials at the nanoscale—chemical, physical, and biological—can differ significantly from those observed in bulk forms (Lee et.al, 2010). When materials are reduced to sizes below 100 nm, their properties can undergo drastic transformations (Kamzin et. al, 2018). As a result, materials can be engineered at the nanoscale to either enhance specific functions or introduce entirely new properties, beyond those associated with changes in size and structure. For example, macromolecules and nanoparticles, which consist of a small number of molecules and range from 1 to 50 nm in size, exhibit distinct physicochemical properties (Roco et.al, 2009). Compared to their bulk counterparts, nanoparticles (NPs) often demonstrate enhanced performance in similar applications.

Has the potential to revolutionize the development of new products, replacing current production methods, reformulating materials and chemicals for improved performance, and promoting more efficient use of resources. These advances can lead to lower material and energy consumption, less environmental harm, and enhanced capabilities for environmental remediation (Subramani et.al, 2012). While reducing resource consumption offers environmental benefits, nanotechnology also presents the opportunity to solve pressing environmental challenges in a more sustainable manner. Applications in this area include the creation of solutions for existing environmental issues, strategies to address the impacts of material and energy interactions with the

environment, and the management of potential risks related to nanotechnology (Poole and Owen, 2003).

Metallic nanoparticles are nanoscale metals, with dimensions ranging from 1 to 100 nm. The existence of metallic nanoparticles in solution was first explored by Faraday in 1857, and Mie later provided a quantitative explanation for their color in 1908 (Dinali et.al, 2017). Today, these nanomaterials can be synthesized and modified with various chemical functional groups, enabling them to interact with antibodies, ligands, and drugs. Metallic nanoparticles find a wide range of applications in the fields of therapy, biotechnology, and as delivery vehicles for genes and drugs (Dabbs and Askay, 2017).

In the real of nanotechnology, metallic nanoparticles have revealed numerous unique properties, opening up new possibilities in the field. With the right functional groups, they can be synthesized and modified to bind with ligands, antibodies, and therapeutic agents (Li et.al, 2004). Notably, metallic nanoparticles possess distinctive features such as surface plasmon resonance and unique optical properties. Noble metals, including silver, iron, and gold, have garnered significant attention from researchers across various disciplines, such as catalysis, photography, and medicine, particularly for their potential as anticancer and antimicrobial agents.

Nanoscale iron particles have garnered significant attention because of their distinctive physical and chemical characteristics. Over time, numerous physical and chemical techniques have been devised for synthesizing these nanostructures. However, many of these methods tend to be costly and may pose risks to human health and the environment. Recently, the synthesis of iron nanoparticles (FeNPs) using plant extracts has gained increasing popularity as an innovative and sustainable alternative, aligning with the principles of green chemistry. This approach replaces traditional chemical compounds and organic solvents with phytochemicals and water-based solutions, offering a more eco-friendly synthesis method. Similar to any chemical and biochemical reaction, factors such as reaction temperature, the concentration of iron precursor, concentration of leaf extract, and reaction time have critical effects on the reaction yield (Jassal et.al, 2016)

Recently, nano- and microstructures have gained applications in various science and technologies (Wang et.al, 2006). Iron nanoparticles (FeNPs) are gaining significant attention as advanced materials because of their distinctive physicochemical characteristics. These include strong catalytic efficiency, notable magnetic properties, minimal toxicity, and effective absorption of microwave radiation. FeNPs are generally grouped into three main categories: iron oxide nanoparticles (IONs), which encompass magnetite (Fe_3O_4), hematite ($\alpha\text{-Fe}_2\text{O}_3$), and maghemite ($\gamma\text{-Fe}_2\text{O}_3$); iron oxide hydroxide (FeOOH) nanoparticles; and zero-valent iron (ZVI) nanoparticles (Rajasekharreddy and Rann, 2014). These nanomaterials have demonstrated versatility across numerous fields such as drug delivery systems (Taniguchi et.al, 1974), magnetically guided targeting (Mijatovic et.al, 2005), cancer hyperthermia therapy (Matsui, 2012), thermal ablation techniques (Anandan et.al, 2016), stem cell sorting and manipulation (Binnig and Rohrer, 2005), gene delivery methods (Bang and Kamat, 2011), enhancement of negative contrast in MRI (Mohan et.al, 2015), food preservation strategies (Rode et.al, 2009), intensification of bioprocesses, antimicrobial treatments, bioseparation processes, ferrofluid development, environmental cleanup efforts, energy storage in lithium-ion batteries, and pigment production (Xing and Dai, 2009). Iron Nanoparticle finds application in environmental remediation, biomedical, defense and aerospace, construction, electronics, healthcare, automotive textiles, agriculture and food. Biomedically, iron nanoparticle especially the oxide (IONPs) has been used in: hyperthermia to cure cancer, drug delivery, anticonvulsant activity of FeNPs

Phyllanthus amarus is a notable plant in the Indian Ayurvedic medicinal tradition, recognized globally for its wide range of therapeutic applications (Patel et.al, 2011). This small, upright annual herb, which reaches a height of approximately 30 to 40 centimeters, belongs to the Euphorbiaceae family. It is commonly referred to as "Carry me go seed" in English, "Eyin Olobe" in Yoruba, "Geeron-Tsuntsaayee" (Bird's millet) in Hausa, and "Enyikwonwa" in Igbo. The plant thrives in damp and shaded environments, with each leaflet on the branch bearing fruit at the base of the flower. Traditional medicine practitioners widely utilize *P. amarus* for various ailments, including malaria, scalp conditions, skin

disorders, gastrointestinal issues, and sexually transmitted infections. According to Guo et.al, 2012, its synonym, *Phyllanthus niruri*, has shown antibacterial activity against pathogens such as *Escherichia coli*, *Klebsiella pneumoniae*, and *Proteus mirabilis*. Additionally, the herb has demonstrated significant efficacy in managing chronic hepatitis B, aiding liver function recovery, and inhibiting the replication of the hepatitis B virus (Xin et.al, 2017). A compound with reverse transcriptase inhibitory function, identified as niruriside, has been extracted from the plant (Qian-Cutrone, 1996). Furthermore, in 1992, *Phyllanthus niruri* was reported to possess HIV-1 reverse transcriptase inhibitory properties (Oguta, 2019). *Phyllanthus amarus* contains a wide array of bioactive compounds, including lignans, terpenes, flavonoids, lipids, benzenoids, alkaloids, steroids, tannins, and saponins. It is known for its multiple pharmacological activities such as antiviral, antibacterial, antiplasmodial, anti-inflammatory, antimalarial, antimicrobial, anticancer, antidiabetic, hypolipidemic, antioxidant, hepatoprotective, neuroprotective, and diuretic effects. Consequently, this study aims to synthesize and analyze iron nanoparticles derived from the leaf extract of *Phyllanthus amarus*. The impact of chemical treatment on the extract and the resulting nanoparticles was investigated using various analytical techniques, including Ultraviolet-Visible (UV-Vis) Spectroscopy, X-Ray Diffraction (XRD), Scanning Electron Microscopy (SEM), and Transmission Electron Microscopy (TEM).

Methods

Materials

Phyllanthus amarus leaves were harvested from the surrounding of SLT building in the premises of federal university of technology, owerri, Nigeria. The plants were identified at the Herbarium of the Department of pharmacognsy at school of pharmacy, Nnamdi Azikiwe University Agulu Campus the following reagents were used in this work; Iron (111) Chloride Hexahydrate ($\text{FeCl}_3 \cdot 6\text{H}_2\text{O}$, 98%), Ethanol, Whatman no.1 filter paper, watch glass, measuring cylinders, Standard flasks, Refrigerator, Mechanical grinder, Sterile sample bottle, Beakers, Distilled- deionized water.

Preparation of leaf extract for phytochemical screening

The leaves of *Phyllanthus amarus* were plucked off the stems, the leaves were collected, washed with de-ionized water, and dried at room temperature for two weeks and thereafter pulverized with mechanical grinder, and transferred into a 250 mL beaker. The grounded leaves were boiled with 100 mL de-ionized water, and filtered with a filter paper on cooling (Xin-Hua et.al, 2017). Phytochemical screening procedures carried out were adopted from (Pattanayak and Nayak, 2013). About 100 g of each of the dried powdered leaves samples were soaked in 200 mL distilled water for 12 hours, the extract was filtered using a Whatman filter paper No. 1, the filtrates were then measured using a measuring cylinder while the extracts were stored separately in a sterile air-tight container.

Green Synthesis of Iron Oxide Nanoparticles using *Phyllanthus amarus*

Iron oxide nanoparticles were synthesized by modified protocol from the previous studies (Kubde and Meenal, 2013). In a typical procedure, 0.01 M $\text{FeCl}_3 \cdot 6\text{H}_2\text{O}$ solution was added to the *Phyllanthus amarus* leaves extract in a 1:1 volume ratio. The reduction reaction occurs immediately after the addition of $\text{FeCl}_3 \cdot 6\text{H}_2\text{O}$. The formation of nanoparticles was evidenced by the appearance of black color in the solution. The Mixture was centrifuged at 4000 rpm for 30 minutes. The UV-vis analysis was immediately carried out to ascertain the synthesis of iron nanoparticles. After the confirmation test, the synthesized Fe_3O_4 -NPs were stored under refrigeration until their characterization. The mixture was later dried using a freeze drier to obtain the Fe_3O_4 -NPs in solid form.

Characterization of Iron Oxide Nanoparticles

UV/Vis Spectrophotometry

Ultraviolet-visible (UV/Vis) spectrophotometry is a technique that measures the absorption or reflection of light within the ultraviolet and visible light spectrum. It is particularly effective in analyzing metal nanoparticles suspended in a solvent or dispersed within an insulating matrix. The method operates on the principle of light interaction with the material, where absorption is attributed to surface plasmon resonance (SPR)—a phenomenon involving the resonance of light waves with free electrons at the surface of the metal

nanoparticles (Maslen et.al, 2004). For this study, the formation of *Phyllanthus amarus*-derived iron nanoparticles (PA-FeNPs) was initially verified by capturing their UV/Vis absorbance spectra within the range of 200–700 nm. The variation in SPR signals over time was monitored using a UV/Vis spectrophotometer. Samples were collected at intervals and placed into quartz cuvettes with a 1 nm resolution setting. Distilled-deionized water served as the blank reference.

X-Ray Diffraction (XRD)

X-ray diffraction (XRD) is a widely adopted analytical technique employed to identify the crystalline structure of unknown solid materials. It plays a vital role in fields such as geology, environmental science, engineering, material science, and biology (Goodhew et.al, 2018). This technique is primarily used to determine the phase composition and structural parameters of crystalline substances. In XRD analysis, the sample material is first finely powdered and uniformly mixed to ensure consistency in analysis. The principle behind XRD involves the constructive interference of monochromatic X-rays that interact with the periodic atomic arrangement in a crystal. These X-rays, generated from a cathode ray source, are filtered to isolate a single wavelength, then collimated and directed at the sample. When the incident rays strike the crystal planes at specific angles that satisfy Bragg's Law ($n\lambda = 2d \sin \theta$), diffraction occurs. This law describes the relationship between the wavelength of the incident X-rays, the diffraction angle, and the distance between the crystal planes. The resulting diffracted rays are detected and recorded, with a range of 2θ values scanned to capture all potential diffraction peaks resulting from the random orientation of the powdered sample.

Scanning Electron Microscope

The scanning electron microscope (SEM) analysis is the same as the transmission electron microscope (TEM) analysis because both have a beam of electrons focused on the specimen. Certain features, such as the electron gun, condenser lenses, and vacuum system, are the same in both instruments, though how the images are produced and magnified are different. The TEM analysis gives information about the internal structure of thin specimens whereas the SEM analysis is used to study the surface, or near the surface, the

structure of specimens. The surface morphology of the nanocluster images was recorded by scanning electron microscope (SEM) of model NOVA NanoSEM, operating at a working distance of 6-13 mm, 5-20 keV accelerating voltage, and 75-80 A emission current.

Transmission Electron Microscope

Transmission Electron Microscopy is a major analytical technique in physics, chemistry, and biological sciences. In nanotechnology the results of TEM analysis play a most important role in imaging morphology and distribution of nanomaterial with high resolution and provide information about the structure, crystallography nature is studied by the diffraction mode. The basic principle of TEM is based on Light Microscope, which uses electrons instead of light and electromagnetic lenses to focus the electrons into a very thin beam rather than glass lenses focus the light. TEM use electrons as a “Light source” and their lower wavelength, high energy makes it possible to get a thousand times better resolution than Light Microscope (Patel et.al, 2011). The electron source present at the top of the microscope emits electrons that travel through a vacuum in the column of the microscope then travels through the specimen to form an image. The specimen is most often an ultrathin section less than 100 nm thick or a suspension on a grid at the bottom of the microscope the unscattered electrons hit a fluorescent screen. This screen gives rise to a “Shadow image” of the specimen with its different parts displayed in varied darkness according to their density.

Results and discussions

Phytochemical Analysis of the Plant Extracts

The phytochemical analysis of the plant extract utilized in this research, as presented in Table 1, revealed the presence of several bioactive compounds, including carbohydrates, reducing sugars, saponins, flavonoids, terpenoids, steroids, and proteins. These compounds played a significant role in both the bioreduction of metal ions and the stabilization (capping) of the newly synthesized nanoparticles. The rapid reaction suggests that the phytochemicals in *Phyllanthus amarus* were sufficient to facilitate the synthesis of PaFeNPs.

Key bio-reducing agents such as citric acid, ascorbic acid, and flavonoids, along with enzymes like reductase and dehydrogenase, are crucial in the reduction of metal ions to their nanoparticle form. These compounds also contribute to stabilizing the nanoparticles, ensuring their structural integrity during and after synthesis (Devatha et.al, 2016).

Table 1. Result of Qualitative Phytochemical Screening of the Plant Extract

<i>Phytochemicals</i>	<i>Presence/Absence</i>
<i>Alkaloids</i>	-
<i>Steroids</i>	+
<i>Flavonoids</i>	+
<i>Tannins</i>	-
<i>Terpenoids</i>	+
<i>Anthraquinone</i>	-
<i>Phlobatannins</i>	-
<i>Cardiac glycosides</i>	-
<i>Reducing sugars</i>	+
<i>Carbohydrates</i>	+
<i>Saponin</i>	+
<i>Coumarin</i>	-
<i>Protein</i>	+
<i>Phenol</i>	-
<i>Amino acids</i>	-
<i>Phytosterol</i>	-

KEY: +Present, -Absent

Characterization of the Iron Oxide Nanoparticles

UV-Vis Properties of Iron Oxide Nanoparticles (FeNPs) under *Phyllanthus amarus*-Influenced Synthesis

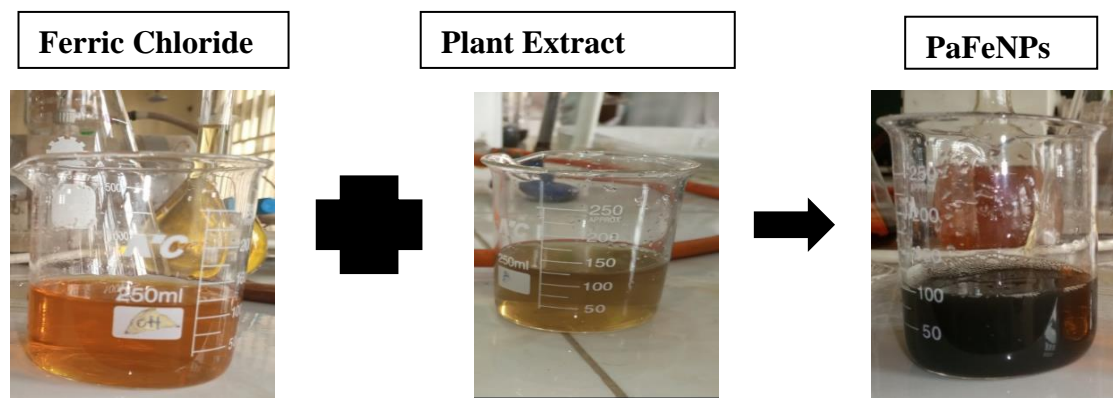


Figure 1. Colour dispersion before and after nanoparticles formation

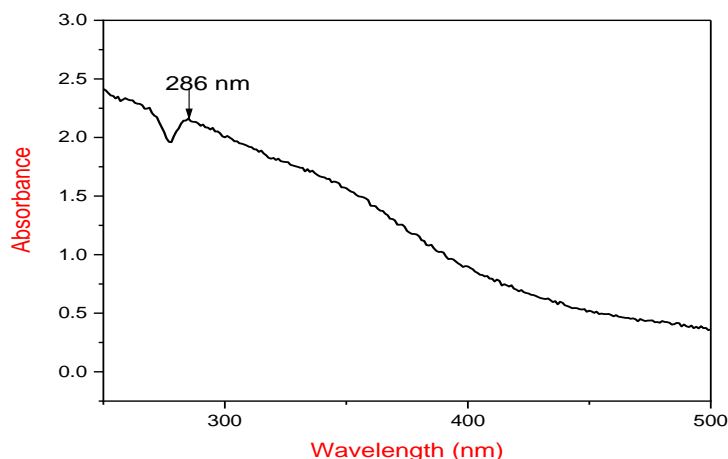


Figure 2. UV-Vis spectra of PaFeNPs

The successful synthesis of PaFeNPs was visually confirmed by an immediate color transformation upon combining the *Phyllanthus amarus* extract with the $\text{FeCl}_3 \cdot 6\text{H}_2\text{O}$ solution. Within seconds of mixing, the solution turned black, indicating the formation of iron nanoparticles (FeNPs), as illustrated in Figure 1. This dark coloration is attributed to the excitation of surface plasmons in the iron nanoparticles, which is a direct indicator of nanoparticle formation. The generation of FeNPs typically involves the initial complexation of iron salts, followed by the stabilization (capping) of the iron particles by phenolic constituents present in the plant extract (Devatha et.al, 2016). The surface plasmon resonance observed in the UV-Vis spectra further confirms the successful reduction of Fe^{3+} ions to form FeNPs. The reduction process of Fe^{3+} ions in the aqueous medium was monitored using UV-Visible spectroscopy, with analysis conducted across a spectral range of 200 to 900 nm to assess the absorbance characteristics of the biologically synthesized FeNPs. A distinct absorption peak appeared at 286 nm (Figure 2), corresponding to the excitation of surface plasmon resonance in the nanoparticles. This finding aligns with previously documented results (Enshirah et. al, 2018).

XRD analysis of PaFeNPs

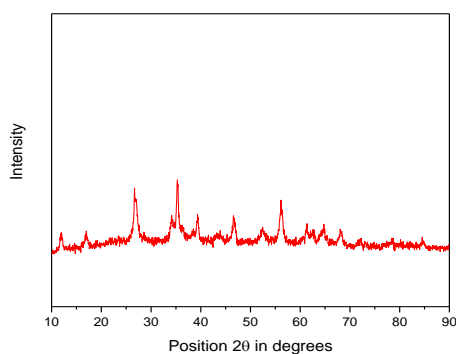


Figure 3. X-ray(powder) diffraction of PaFeNPs

X-ray diffraction (XRD) analysis was utilized to assess the crystalline nature and particle size of the synthesized PaFeNPs. The XRD pattern displayed sharp diffraction peaks (Figure 3), indicating that the nanoparticles were highly crystalline. Additionally, the noticeable broadening of some peaks suggested the formation of nanocrystals with very small dimensions. Distinct diffraction peaks were observed at angles of 27°, 35°, 39°, 46°, 52°, 56°, 64°, and 67°, which correspond to the (220), (311), (400), (422), (511), (440), (620), and (533) planes, respectively. These diffraction peak positions and their relative intensities align closely with the standard pattern of an inverse spinel structure as documented in JCPDS card No. 39-1346, thereby confirming the presence of Fe_3O_4 nanocrystals in the sample. Using the Scherrer equation, the average crystallite size (D) of the nanoparticles was estimated to be approximately 9.13 nm (Herlekar et.al, 2014). The high crystallinity and nanometric scale of the Fe_3O_4 particles suggest excellent stability and enhanced magnetic properties, which are critical for applications such as targeted drug delivery, magnetic resonance imaging (MRI), and environmental remediation. The inverse spinel structure further supports the potential for strong magnetic behavior and efficient catalytic performance.

SEM and TEM

b

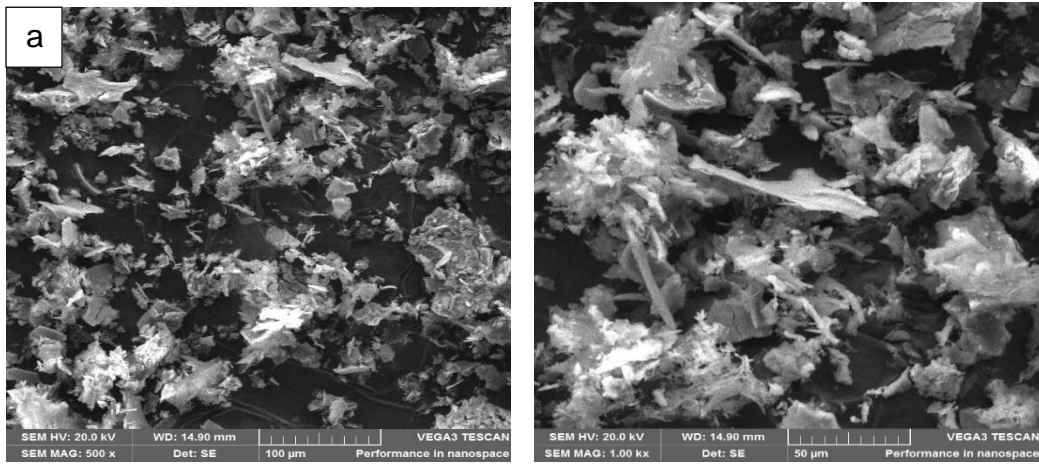


Figure 4. (a and b) SEM images of PaFeNPs

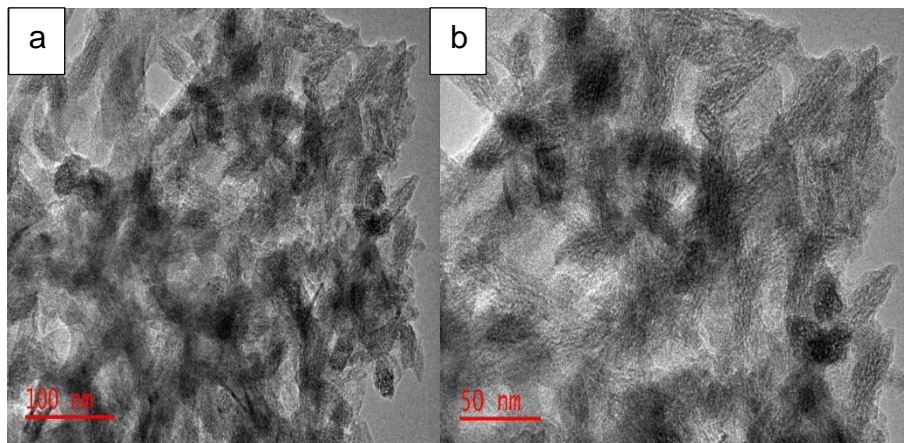


Figure 5. (a and b) TEM images of PaFeNPs

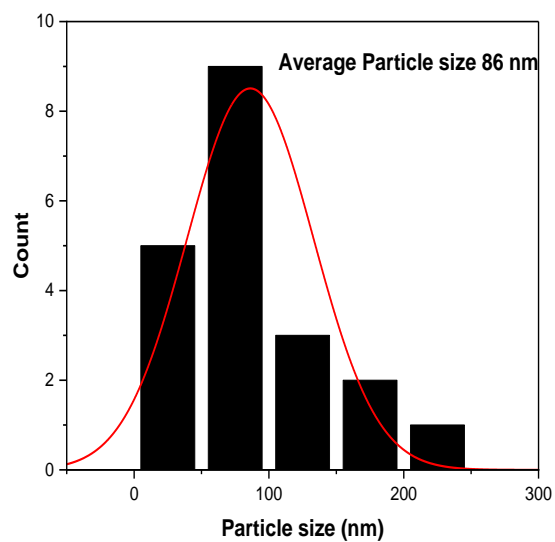


Figure 6. Particles size distribution PaFeNPs

Scanning Electron Microscopy (SEM) was employed to examine the surface characteristics of the synthesized nanoparticles. As illustrated in Figures 4.6a and b, the SEM images reveal that the PaFeNPs are moderately clustered and display a non-uniform, irregular morphology. This morphological irregularity may enhance the surface area and reactivity of the nanoparticles, which is advantageous for catalytic and adsorption-based applications. Further insights were gained from Transmission Electron Microscopy (TEM), shown in Figures 4.7a and b, which confirmed the presence of particle aggregation. This aggregation suggests strong interparticle connectivity and a predominantly rod-like or cubic structural appearance, features that can improve magnetic behavior and facilitate targeted applications such as magnetic separation or drug delivery. The tendency of FeNPs to cluster is primarily due to magnetic dipole–dipole interactions between the individual iron particles [45]. Using image analysis software, the particle size observed in the TEM image was measured to be approximately 86.2 nm, as demonstrated in Figure 5.

Conclusion

The characterization results obtained through UV-Visible spectroscopy, X-ray diffraction (XRD), Transmission Electron Microscopy (TEM), and Scanning Electron Microscopy (SEM) verified the successful formation of iron oxide nanoparticles. These findings demonstrate that *Phyllanthus amarus* functions effectively as both a reducing and stabilizing agent in the conversion of Fe³⁺ ions to iron nanoparticles. This eco-friendly approach offers a sustainable, cost-efficient, and easily accessible method for nanoparticle synthesis. The resulting nanoparticles fall within the nanoscale range of 1–100 nm, reinforcing the feasibility and practicality of this green synthesis route (herlekar et.al, 2014). Future work will focus on evaluating the catalytic, antimicrobial, and dye-degradation efficiencies of these nanoparticles in real-world environmental and biomedical applications, as well as optimizing synthesis parameters to enhance yield and functional performance.

Contribution to Knowledge

Since the synthesized phyllanthus amarus mediated iron oxide nanoparticles were successfully used in degradation of crystal violet dyes in this research

work, same will be encouraged to be used by large organizations and industries in treatment of waste water.

Recommendation

The study of the antimicrobial properties of the synthesized PaFeNPs should be carried out. Effect of desorption of CV dye from the surface of the PaFeNPs should- be confirmed by measuring the pH of the CV dye solution. Further study on the use of green plants for the synthesis of iron oxide nanoparticles should be encouraged to reduce the use of toxic chemicals that could degrade our environment.

LIST OF REFERENCE

- Adewoye, S.O. and Lateef, A. (2004): Assessment of the microbiological quality of *Clarias gariepinus* exposed to an industrial effluent in Nigeria. *The Environmentalist (now Environment Systems and Decisions)*, 24: 249-254.
- Anandan, S., Hebalkar, N., Sarada, B.V. and Rao, T.N. (2016): Nanomanufacturing for aerospace applications. In: *Aerospace materials and material technologies*. Singapore: *Springer*. p. 85–101.
- Aghdam, M. T. B., Mohammadi, H. and Ghorbanpour, M. (2016): Effects of nanoparticulate anatase titanium dioxide on physiological and biochemical performance of *Linum usitatissimum* (Linaceae) under well-watered and drought stress conditions. *Braz Journal Bot*, 39:139–46.
- Bang, J. H. and Kamat, P. V. (2011): CdSe quantum dot-fullerene hybrid nanocomposite for solar energy conversion: electron transfer and photoelectrochemistry. *ACS Nano*. 5(12):9421–7.
- Binnig, G. and Rohrer, H. (2005): Scanning tunneling microscope. *Scientific American*. 253:50–6.
- Brans, W.L., Dereux, A. and Ebbesen, T.W., (2003): *Nature*, 424, 824.
- Dabbs, D.M. and Aksay, I.A. (2017): Self-assembled ceramics produced by complex-fluid templation. *Ann Rev Phys Chem*, 51(1):601–22.

- Devatha, C.P., Kumar, A. and Katte, S.Y. (2016): Green synthesis of iron nanoparticles using different leaf extracts for treatment of domestic waste water. *J. Clean. Prod.*, 139, 1425–1435.
- Dinali, R., Ebrahiminezhad, A., Manley-Harris, M., Ghasemi, Y. and Berenjian, A. (2017): Magnetic immobilization of bacteria using iron oxide nanoparticles. *Biotechnology Letters*. <https://doi.org/10.1007/s10529-017-2477-0>.
- Ebrahimi, N., Mansoori, G. A., (2014): Reliability for drug targeting in cancer treatment through nanotechnology (a psychometric approach). *International Journal of Medical Nano Research*. 1:1–5.
- Enshirah, D., Amel, T. and Eman, A. (2018): Green synthesis of iron nanoparticles by *Acacia nilotica* pods extract and its catalytic, adsorption, and antibacterial activities. *Applied Sciences*, 8(10): 5-17. <https://doi:10.3390/app8101922>.
- Goodhew, P. J., Humphreys, J., and Beanland, R. (2018): *Electron Microscopy and Analysis, Taylor and Francis, London and New York*. 4(3), 51-53.
- Guo, J., Wang, R., Tjiu, W. W., Pan, J. and Liu, T. (2012): Synthesis of Fe nanoparticles@ graphene composites for environmental applications. *Journal of Hazardous Materials*, 225, 63–73.
- Herlekar, M., Barve, S., and Kumar, R. (2014): Plant-mediated green synthesis of iron nanoparticles. *Journal of Nanoparticle Research*, 1–9.
- Heath, J.R., O'Brien, S.C., Zhang, Q., Lui, Y., Curl, R.F., Tittel, F.K. and Smalley, R.E. (2005): Lanthanum complexes of spheroidal carbon shells. *Journal Am Chem Soc*, 107:7779–80.
- Iijima S, Brabec C, Maiti A, Bernholc J. Structural flexibility of carbon nanotubes. *Journal of Chemical Physics*, 104(5):2089–92.
- Jassal, V., Shanker, U. and Gahlot, S. (2016): Green synthesis of some iron oxide nanoparticles and their interaction with 2-amino, 3-amino and 4-aminopyridines. *Materials Today*, 3(6), 1874–1882.]
- Kamzin, A.S., Valiullin, A.A., Khurshid, H., Nemat, Z., Srikanth, H., Phan, M.H. and Mössbauer. (2018): Studies of Core–Shell FeO/Fe₃O₄ Nanoparticles. *Phys. Solid State*, 60, 382–389.

- Kubde, P.L. and Meenal, S. (2010): *Lagenaria siceraria*: Phytochemistry, pharmacognosy and pharmacological studies. *Rep Opi.*, 2(3): 91-98.
- Lee, J., Mahendra, S. and Alvarez, P. J. J., (2010): Nanomaterials in the construction industry: a review of their applications and environmental health and safety considerations. *ACS Nano*, 4(7):3580–90.
- Li, Y., Lee, N.H., Hwang, D.S., Song, J.S., Lee, E.G. and Kim, S.J. (2004): Synthesis and characterization of nano titania powder with high photoactivity for gas-phase photo-oxidation of benzene from TiOCl_2 aqueous solution at low temperatures. *Langmuir*, 20(25):10838–44.
- Machado, S., Pacheco, J.G., Nouws, H.P., Albergaria, J.T. and Delerue-Matos, C. (2015): Characterization of green zero-valent iron nanoparticles produced with tree leaf extracts. *Science of the Total Environment*, 15(533), 76–81.
- Mijatovic, D., Eijkel, J.C.T. and Berg, A. (2005): Technologies for nanofluidic systems: top-down vs. bottom-up—a review. *Lab Chip*, 5:492–500.
- Matsui, S. (2012): Focused-ion-beam chemical-vapor-deposition (FIB-CVD). In: Encyclopedia of nanotechnology.: Dordrecht Springer. 18.
- Mohan, K., Gokhale, M., Ravindra, K.P. and Somani, R. (2015): Fullerenes: chemistry and its applications. *Mini Rev Org Chem*, 12:355–66.
- Maslen, E.N., Fox, A.G. and O’Keefe, M.A. (2004): *X-ray Scattering*, in: E. Prince (Ed), *International Tables for Crystallography*, Kluwer Academic, Dordrecht.
- Nguyen, P. and Berry, V. (2012): Graphene interfaced with biological cells: opportunities and challenges. *Journal Phys Chem Lett.* 3:1024–9.
- Oguta, T., (2019): HIV-1 reverse transcriptase inhibitor from *Phyllanthus niruri*. *AIDS Human Retroviruses.* 8 (11): 1937-1994.
- Patel, J.R., Tripathi, P., Sharma, V., Chauhan N. S. and Dixit V. K. (2011): *Phyllanthus amarus*: ethnomedicinal uses, phytochemistry and pharmacology: a review *Journal Ethnopharmacol*, 138:286–313.
- Pattanayak, M. and Nayak, P.L. (2013): Ecofriendly green synthesis of iron nanoparticles from various plants and spices extract. *J. Plant Anim. Environ. Sci.*, 3, 68–76.

- Pattanayak, M.K., Monalisa, L. and Nayak, P.L. (2013): Green synthesis and characterization of zero valent iron nanoparticles from the leaf extract of *Azadirachta indica* (Neem). *World of innovative research*. 2(1), 06-09.
- Poole, J.C.P., and Owens, F.J. (2003): Introduction to nanotechnology. Introduction to Technology & engineering. Hoboken, NJ John Wiley & Sons
- Qian-Cutrone, J. (1996): Niruriside a new HIV reverse binding inhibitor from *Phyllanthus niruri* J. *Nat. Prod.* 59 (2): 196-199.
- Ramya, M., and Sylvia, M. S. (2012): Green synthesis of silver nanoparticles. *Int J Pharm Med. Biol. Science*, 1(1): 10-31.
- Rajasekharreddy, P. and Rani, P. U. (2014): Biofabrication of Ag nanoparticles using *Sterculia foetida* L. seed extract and their toxic potential against mosquito vectors and HeLa cancer cells. *Materials Science and Engineering: C*, 39, 203–212.
- Roco, M. C., Williams, R.S. and Alivisatos, P. (2009): editors. Nanotechnology research directions: vision for nanotechnology in the next decade. IWGN workshop report, WTEC, Loyola College in Maryland.
- Rode, A.V., Hyde, S.T., Gamaly, E.G., Elliman, R.G., McKenzie, D.R., Bulcock, S. (2009): Structural analysis of a carbon foam formed by high pulse-rate laser ablation. *Applied Phys A*. 69: S755–8.
- Sanchez, V.C., Jachak, A., Hurt, R.H. and Kane, A.B. (2012): Biological interactions of graphene-family nanomaterials: an interdisciplinary review. *Chemical Research in Toxicology*, 25(1):15–34.
- Shahwan, T., Abu Sirriah, S., Nairat, M., Boyacı, E., Eroğlu, A. E., and Scott, T. B. (2011): Green synthesis of iron nanoparticles and their application as a Fenton-like catalyst for the degradation of aqueous cationic and anionic dyes. *Chemical Engineering Journal*, 172(1), 258–266.
- Subramani, K., Ahmed, W., Hartsfield, J. K., (2012): editors. Nanobiomaterials in clinical dentistry. Elsevier Inc.
- Taniguchi, N. Arakawa, C. and Kobayashi, T. (1974): On the basic concept of nano-technology. In Proceedings of the International Conference on Production Engineering, Tokyo, Japan.

- Wang, B., Kra, I. P. and Thanopoulos, I. (2006): Docking of chiral molecules on twisted and helical nanotubes: nanomechanical control of catalysis. *Nano Letter*, 6(9):1918–21.
- Xing, Y., Dai, L., (2009): Nanodiamonds for nanomedicine. *Nanomedicine*, 4(2):207–18
- Xin-Hua, W., Chang-Qing, L., Xing-Bo, G., Lin-Chun, F. A. (2017): comparative study of *Phyllanthus amarus* compound and interferon in the treatment of chronic viral hepatitis B *Southeast Asian J. Trop. Med. Public Health.*,32 (1): 140-142.